Fringe tracking at VLTI: status report

Jean-Baptiste Le Bouquin[a], Roberto Abuter[b], Bertrand Bauvir[b], Henri Bonnet[b], Pierre Haguenauer[a], Nicola di Lieto[b], Serge Menardi[b], Sébastien Morel[a], Fredrik Rantakyrö[a], Markus Schoeller[b], Anders Wallander[b], Stefan Wehner[a]

[a] European Southern Observatory, Casilla 19001, Santiago 19, Chile
[b] European Southern Observatory, Garching, Germany

ABSTRACT

FINITO (the VLTI three beam fringe-tracker) has been offered in September 2007 to the astronomical community for observations with the scientific instruments AMBER and MIDI. In this paper, we describe the last improvements of the fringe-tracking loop and its actual performance when operating with the 1.8m Auxiliary Telescopes. We demonstrate the gain provided to the scientific observations. Finally, we discuss how FINITO real-time data could be used in post-processing to enhance the scientific return of the facility.

Keywords: Optical Long Baseline Interferometry ; Fringe Tracking ; VLTI ; FINITO

1. INTRODUCTION

The major difficulty of optical interferometry from the ground is the Optical Path Difference (OPD) introduced by the atmospheric turbulence. Its random amplitude is much larger than the fringe spacing, prohibiting any meaningful measure of fringe contrast (also called visibility) and phase, which are the quantities of astrophysical interest. Practically, fringe blurring is avoided, either by reducing the integration time to a few milliseconds, which prevents observations of faint targets; or by using a dedicated fringe-tracking facility, the purpose of which is to stabilize fringes by measuring and correcting the OPD in real-time.

FINITO (Fringe-tracking Instrument of NIce and TOrino) has been developed in collaboration between ESO and the Astronomical Observatory of Torino to provide a first-generation, on-axis, fringe-tracking facility for the scientific instruments AMBER (3-beam, JHK-bands) and MIDI (2-beam, N-band) from the Very Large Telescope Interferometer (VLTI, see Haguenauer et al. in this proceeding). A strong effort from ESO[1] allowed offering FINITO to the astronomical community in September 2007 for operations with the 1.8m Auxiliary Telescopes (ATs) and in October 2008 for operations with the 8.2m Unit Telescopes (UTs). In the past, several papers have presented the FINITO design and expected performance,[1–3] while no summary of actual performance and operational experience gained on sky has been published yet. This is the purpose of this paper.

In Section 2 we briefly recall the FINITO beam-combination concept, and the algorithms used to convert the raw fringe signal into phase, group-delay and Signal to Noise Ratio (SNR). We detail how these quantities are used to control the fringe-tracking loop through the OPD Controller machine (OPDC). Section 3 describes the improvements added recently to the FINITO/OPDC in order to tackle different operational issues and increase the performance. We also list the remaining known difficulties. Section 4 focus on performance. We first presents the current FINITO working range, based on statistic of observations made under various atmospheric conditions. We then detail the impact of fringe-tracking on the AMBER data quality and our operational experience of MIDI with FINITO. Finally, Sec. 5 presents perspectives opened by our new capability to log the FINITO/OPDC real-time data. These studies are still under progress, so we present only qualitative results. Paper finishes with brief conclusions and recommendations concerning possible hardware improvements.

2. FRINGE-TRACKING AT VLTI

A sketch of FINITO/OPDC fringe-tracking concept at VLTI is displayed in Fig. 1.

Send correspondence to J.B Le Bouquin: E-mail: jlebouqu@eso.org, Phone: +56 2 463 3087
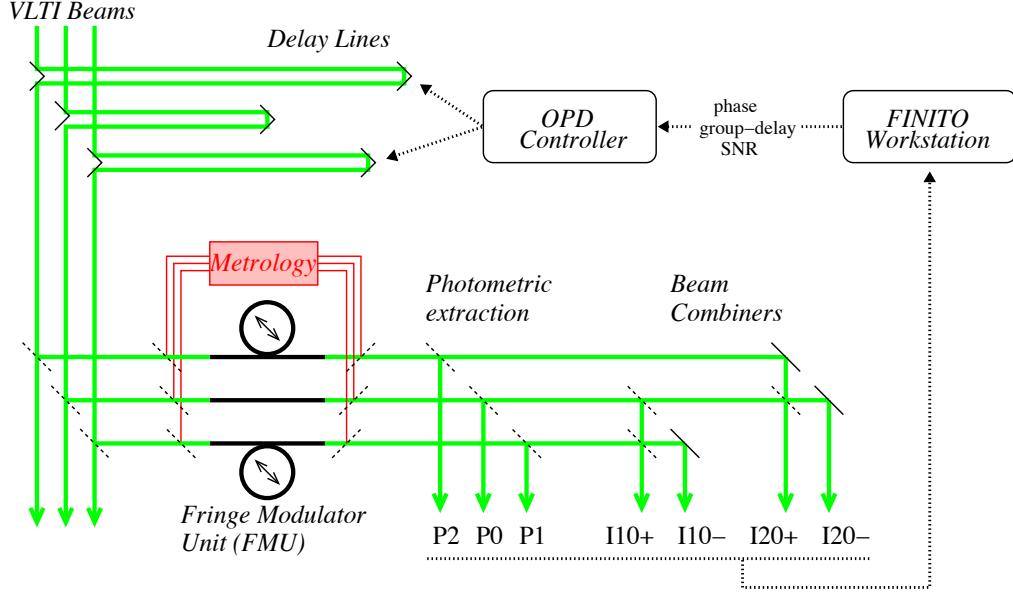
Figure 1. Sketch of the fringe-tracking concept when using FINITO/OPDC at the VLTI. Optical beams (solid green lines) are routed to the FINITO beam-combiner, where photometric extraction and interferometric combination is performed by the mean of semi-transparent devices (dashed black lines) and mirrors (solid black lines). The temporal OPD modulation created by the stretched fibers (FMU) is linearized with an internal metrology system (red). The raw real-time data flow (lower dotted lines) is converted into fringe phase, group-delay and SNR. These signals (upper dotted lines) are used by the OPD Controller to pilot the Delay Lines in closed loop.

2.1 FINITO beam-combiner design

FINITO combines in H-band two pair of baselines from a telescope triangle. Optical Path Length of two of the three beams are modulated internally using a piezo driven expansion ring changing the length of the fibers. The linearity of the modulation is ensured by an auxiliary metrology system operating at 1312 nm. We generally use a triangular modulation of 5 H-band fringes in amplitude peak-to-peak and with a 4 samples per fringe. Each modulation ramp is hereafter called a scan. Photometric signals are extracted by Glan-Taylor polarizers. The transmitted polarization component is fed to a three-way beam combiner. The central beam (labelled 0) is split in equal intensity fractions, and then combined with the modulated beams (respectively 1 and 2). This produces two pairs of complementary interferometric outputs (π phase difference), for the combination 0-1 and 0-2 respectively. The 3 photometric signals (P_1, P_0, P_2) and the 4 interferometric signals ($I_{10}^+, I_{10}^-, I_{20}^+, I_{20}^-$) are routed to a Rockwell PICNIC camera, which is read at frequency between 500Hz and 2kHz.

2.2 Real time data processing

Raw data are processed in real-time: the two interferometric outputs are corrected and calibrated from the photometric fluctuations by the classical following formula (here for baseline 10):

$$C_{10}^+ = \frac{I_{10}^+ - \kappa_{1\to10^+} P_1 - \kappa_{0\to10^+} P_0}{2\sqrt{\kappa_{1\to10^+} \kappa_{0\to10^+} P_1 P_0}} \qquad\qquad C_{10}^- = \frac{I_{10}^- - \kappa_{1\to10^-} P_1 - \kappa_{0\to10^-} P_0}{2\sqrt{\kappa_{1\to10^-} \kappa_{0\to10^-} P_1 P_0}} \qquad (1)$$

The κ matrix is the internal transmission ratio between the photometric and the interferometric outputs. It is calibrated before each observation by measuring the flux at the outputs while feeding one input beam at a time. Then, a phase reconstruction algorithm is used to demodulate the observed signals C_{10}^+ and C_{10}^-, that is to restore the input phase and group-delay by combining several samples acquired at different dates. Currently, phase and group-delay can be estimated with 3 different estimators, derived from the classical ABCD algorithm. Even if detailed mathematical description is out of the scope of this paper, we describe the assumptions and basic concepts of each of them:

fastAB : The instantaneous fringe phase and contrast are estimated at each IRACE readout i by exploiting the π phase shift between the fringe signals. To do so, a classical ABCD estimator is applied to the quantities $C_{10}^-(i-1)$, $C_{10}^-(i)$, $C_{10}^+(i-1)$ and $C_{10}^+(i)$. At the end of each scan, the group-delay is evaluated computing the barycenter of the contrast curve over the OPD ramp.

ABCD : The complementary signals are subtracted: $C_{10} = C_{10}^- - C_{10}^+$. This enhances the SNR and removes all the correlated noises between the two outputs, like photometric residuals. A classical ABCD estimator is applied to the quantities $C_{10}(i-3)$, $C_{10}(i-2)$, $C_{10}(i-1)$ and $C_{10}(i)$. The group-delay is evaluated computing the barycenter of the contrast at the end of each scan.

CSPA (Constant Speed Phase Algorithm): The previous algorithms implicitly rely on the assumption that the phase did not change during the acquisition of the samples used for the reconstruction. In presence of bad coherence time or mechanical vibrations of optical elements, the constant phase assumption is not verified and the algorithms fail to reconstruct a realistic phase. To tackle this issue, the CSPA algorithm assumes that the first temporal derivative of the phase was constant during the acquisition and does not exceed $\pi/2$ per cycle. Outputs of the algorithm are contrast, phase and phase-speed. The group-delay is computed at the end of each scan, by comparing the actual fringes to a reconstruction based on the phase estimations.

With all algorithms, the SNR is computed dividing the measured contrast with the contrast measured in absence of fringes, the latter being estimated before the fringe acquisition. Operational experience showed that the CSPA algorithm is the most robust to external OPD perturbations like mechanical vibrations. It is used by default for all operation.

2.3 The OPD Controller

The FINITO output quantities (SNR, phase, group-delay) are forwarded to the OPD Controller. This computer implements the real-time control law of the fringe tracking loop and send the so-called "real-time offset" to the corresponding Delay Line. Initially, a three state machine has been implemented to handle the initial fringe search and the recovery after fringes have been lost (see left panel of Fig. 2). During a search, fringes are considered "found" and loop is closed when the SNR reaches the *det* threshold. This level is typically higher than 4 to avoid false detection. Loop freezes as soon as the SNR goes below *open* (typically 2.5), to avoid sending noise. In the following 20ms loop may close again as soon as SNR reaches *close* (typically 3 to 5). Otherwise, if SNR remains below *close* for more than 20ms, fringes are declared "lost" and a recovery search is initiated.

When fringe-tracking loop is closed, and each time the absolute value of the group-delay averaged over 20 scans is larger than π, an OPD kick of amplitude 1−fringe is send to the Delay Lines while the loop opens temporally. This ensures to maintain the group-delay as small as possible while tracking on the phase. This also allows to recover the fringe of maximum contrast even if fringe-tracking loop has closed away from the packet center.

3. RECENT IMPROVEMENTS AND REMAINING ISSUES

3.1 Improved OPDC state machine

The OPD Controller state machine is a key element because it contains all the intelligence of the tracking loop. Spending time to optimize it is a worthwhile effort. Initially, a constant value was expected for the detection threshold used during a search (*det*∼10, relatively high to avoid false detection and be sure to lock close to the packet center). Yet, on a bright and unresolved star this threshold is reached on fringes with very small contrast. So fringe-tracking loop generally closes far away from the packet center, up to several tens of fringes. On such faint fringes, the loop is highly unstable and never stays close sufficient time so that the group-delay correction (1−fringe kicks) could recover the center of the fringe packet. The state machine oscillates between state "search" and "lock", providing very poor loop stability and performance. On the other hand, a SNR of 10 may never be achieved on a faint or highly resolved star. Fringes are not detected even if easily seen with unaided eyes!
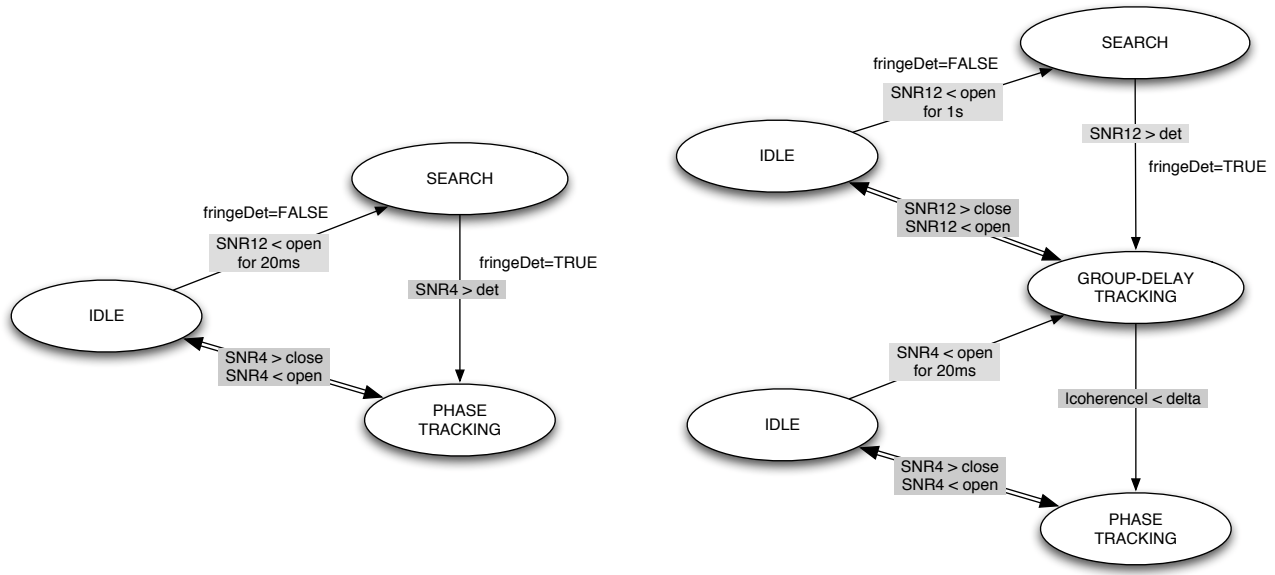
Figure 2. Old (left) and new (right) OPDC state machine. The old state machine generally used thresholds level of: *open*=2.5, *close*=3 and 5<*det*<40 (adjusted to the maximum observed SNR, e.g. the center of the fringe-packet). The improved state machine uses thresholds level of: *open*=2.5, *close*=3, *det*=6 (whatever the target flux and visibility), and *delta*=2π. The raw SNR value is averaged over 4 or 12 samples (SNR4 and SNR12) to reduce sensitivity to measurement noise.

To tackle this issue, we improved the OPDC state machine by implementing a two stage logic: loop is first closed in group-delay tracking only, and *then* on the fringe phase (see Fig. 2, right). Rules to rise and degrade states are similar to the previous state machine, expect for the transition group-tracking to phase-tracking which uses a criteria based on the group-delay value. First, the phase-tracking always starts around the fringe-packet center defined as group-delay=0, even on a bright and unresolved stars, and without having to artificially increase the *det* threshold. Secondly, since a small value of *det*=6 is used by default, fringes are detected on fainter or highly resolved targets. Even if phase-tracking loop never really starts because the observation is too challenging, fringes are at least kept around by the group-delay tracking loop.

3.2 Improved recovery after a flux dropout event

The spatial filtering improves the fringe contrast by transforming the wavefront errors over the pupil into fast fluctuation of the injected flux. Occasional flux dropout are generally not critical for scientific instruments, where frame selection can be applied during the a-posteriori data reduction process. Yet, the situation is more complicated in the case of a fringe-tracker like FINITO. Figure 3 shows a typical fringe-track obtained with the old state-machine in a regime of numerous flux dropout. Over 25s, fringes have been declared "lost" 5 times, triggering recovery searches. Interestingly, fringes have always been recovered very close to where they have been lost. Moreover, and it is clear on the first event, fringes were not really lost when the recovery search started (SNR∼2). But they have been pushed away by the search for several seconds (SNR∼1), and finally recovered at the same position.

The new state machine described in previous section significantly improved the recovery time. First, a smaller *det* threshold is used by default, so the fringes have better chance to be re-detected quickly before being pushed away. Then, when phase-tracking loop failed, OPDC tries the group-tracking loop instead of immediately triggering a search. At least, fringes are kept around until the conditions improve again so that phase-tracking can re-start. Finally, we chose an idle time of 1s for the group-tracking loop before triggering the recovery search, based on our experience that fringes are generally not lost because of a strong atmospheric OPD kick, but because of flux dropouts.
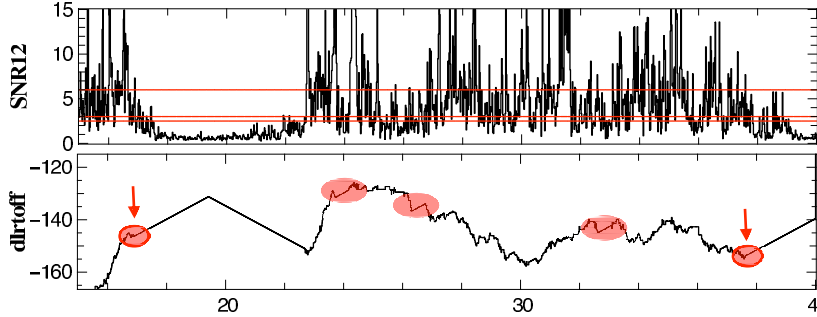
Figure 3. Typical fringe-track sequence obtained with the old state-machine in a poorly injected regime, that is with numerous flux dropouts. Top is the instantaneous SNR, with *open*, *close* and *det* thresholds (horizontal lines). Bottom is the Delay Lines tracking offsets, measured in H-band fringe size (1.65μm). Time is in second. During the track, fringes have been declared "lost" five times (circles). Three events were recovered quickly by the OPDC, while two events took more than 5s (first and last).

With the current version of the OPDC state machine, operational decisions are simple: (i) No parameters need to be adjusted by the user. (ii) State machine informs the user in real-time about the fraction of time spend in group-tracking and phase-tracking. (iii) Even if phase-tracking is at the limit, fringes are never lost thanks to the "security" provided by the group-tracking. (iv) If group-tracking is at the limit, user should forget about phase-tracking since this means an average SNR below 6, and/or numerous flux dropout.

3.3 Remaining issues concerning control

Chromatic dispersion is still not taken into account by the FINITO/OPDC tracking loop. Because the Delay Line tunnels of VLTI are not under vacuum, the difference of air path encountered by the two interferometric arms introduces a chromatic phase dispersion (also called Longitudinal Atmospheric Dispersion), especially when pointing at high airmass. First, dispersion reduces the maximum fringe contrast, leading to degraded performance. Secondly the fringe packet is enlarged in OPD, so group-delay estimation is more noisy. As a consequence, fringe jumps are more difficult to detect and correct. Finally, if the phase-tracking loop is perfectly closed, the group-delay slightly changes with time (difference between group and phase velocities). This differential velocity is clearly seen in Fig. 4 where the phase is well canceled during about 30s (top), while the group-delay increases at constant rate during the whole track. The slow group-delay motion is not a problem by itself because we never integrate more than 10s on the science instrument. However, when the difference between phase and group-delay is about half a fringe, the loop has two equivalent positions of equilibrium (phase=0 and group-delay=$-\pi$, or phase=0 and group-delay=$+\pi$). This results into numerous OPD jumps of $\sim 1.62\mu$m, that are killers when observing with AMBER in J or K bands (1.3μm and 2.2μm respectively).

Important issues also affect the group-delay tracking loop, where large OPD offsets are send at each end of scan. The Delay Line takes about 3ms to handle an offset of few fringes, which disturbs the fringe contrast of several samples in the following scan. The group-delay estimation (based on the contrast) is systematically biased and the loop sometime enters an oscillating regime until it breaks. A simple solution would be to spread the OPD correction over the complete scan. Contrast would be slightly degraded, but on an homogeneous manner over the whole scan, and so without disturbing the group-delay estimation. This is currently under investigation. Concerning the group-delay tracking loop, we also plan to implement a more evolved PID controller (Proportional Integrator Derivative) instead of the simple gain used by now.

Yet, the main difficulty for fringe-tracking at VLTI remains the mechanical vibrations of optical elements. These vibrations are not seen in auto-collimation mode, proving that Delay Lines tunnel and VLTI laboratory are quiet enough. Concerning the UTs, it has been proved that the most important source of vibrations are the instruments placed at the Nasmyth and Cassegrain focus. We emphasize here that these vibrations not only impact the VLTI but also current and incoming Adaptive Optics experiments (NaCo, Sphere...). Hardware changes, accelerometers, and vibration tracking algorithms have been required to obtain reasonable fringe-tracking performance when observing with the UTs (see papers of Pierre Haguenauer and Nicola di Lieto in this proceeding).
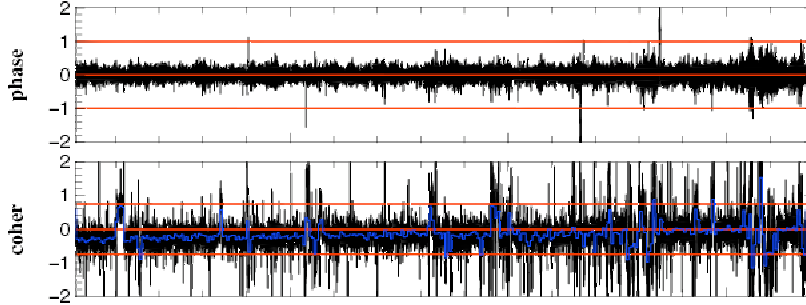
Figure 4. Typical FINITO fringe-track sequence obtained in the high SNR regime, when observing at high airmass. The phase (top) and group-delay (bottom) are displayed in H-band fringe size (1.62μm). The phase is well tracked over the 30s, while the group-delay is slightly changing with time because of the Longitudinal Atmospheric dispersion. The blue curve is a moving average of the group-delay.

Concerning the ATs, the situation is much less dramatic, and vibrations are mainly driven by wind larger than $\sim$10m/s.

4. OPERATING RANGE AND PERFORMANCE

4.1 Operating range

Defining the weather conditions in which fringe-tracking works properly is critical for optimal use of the night-time at Paranal observatory. First the number of observations to be scheduled can be adjusted to the expected usable fraction of time. Secondly, it allows the night-time operator to decide whether to execute or not an observation based on the current weather conditions.

Figure 5 shows the FINITO performance, expressed as phase RMS over a $\sim$1min exposure, versus the observed flux, the seeing, and the coherence time τ_0. The two lasted quantities are estimated at Paranal observatory by a DIMM working in the visible range. All data have been recovered by browsing the automatic logs with the powerful `autrep` system. Unfortunately, we were not able to recover the fringe visibility since it was not written in the automatic logs (it has been added recently). This may explain part of the vertical dispersion of Fig. 5, meaning that bad performances obtained in good conditions may be related to observations of highly resolved sources with small fringe contrast. Note also that the point density may be biased by astronomer's decisions: in case of good seeing, the operator may try a challenging faint object ; while in case of bad seeing, he will concentrate on very bright and unresolved targets only. Yet, several interesting points can be learnt. First channel 10 is less efficient than channel 20, possibly because of known difference in focus adjustment of the injection optic of beam 1 in comparison to beam 0 and 2. this has been corrected recently by adjusting all FINITO fibers to the new VLTI focus reference. This assumption might thus be wrong now, and we should keep monitoring this difference in the future. Secondly, τ_0 appears to be a better metric than the seeing when deciding to go or not for an observation requiring fringe-tracking. This is an important result for short-term scheduling by night-time astronomers. Finally, the best RMS obtained are around 0.25rad in the H-band, which corresponds to $\sim$70nm. This is well within the specification of 150nm.[2] These good performance are achievable over a large range of weather conditions, even if not *guaranteed*.

Based on this study, we defined the weather related working conditions to be: seeing<1.2as and τ_0>3ms. Considering the fringe contrast, we never manage to track on fringe with visibility smaller than V$\sim$5% because of large photometric residuals, even in the quantity $C_{10} = C_{10}^- - C_{10}^+$ used by the ABCD and CSPA algorithms. It is not clear to us why the photometry is not perfectly canceled, but we suspect the fact that photometric and interferometric signals come from different polarizations extracted after a single mode polarization-maintenance fiber (coupling efficiency of both polarization states may be different and not perfectly correlated).

Based on operational experience, the limiting magnitude on the 1.8m Auxiliary Telescopes is Hmag$\sim$6 (correlated flux), when observing with weather conditions within the 10% best conditions at Paranal. This result is far from the predicted limiting magnitude claimed by Gai et al., of the order of Hmag$\sim$10.[2] However, the
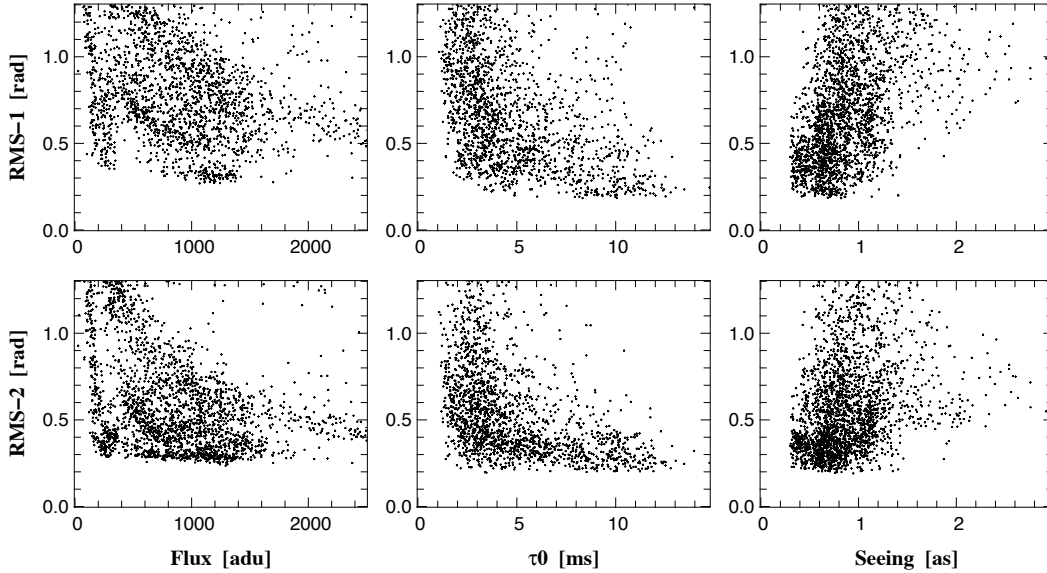
Figure 5. Fringe-tracking performance (phase RMS in rad) of both FINITO channels versus the flux on beam0 (common beam to tracked baselines), the coherence time, and the seeing. All points have been obtained with FINITO running at 1kHz. Data have been extracted from the automatic log with the `autrep` tool, ranging for about 4 months of observations. Unfortunately, the fringes contrast was not stored at that time.
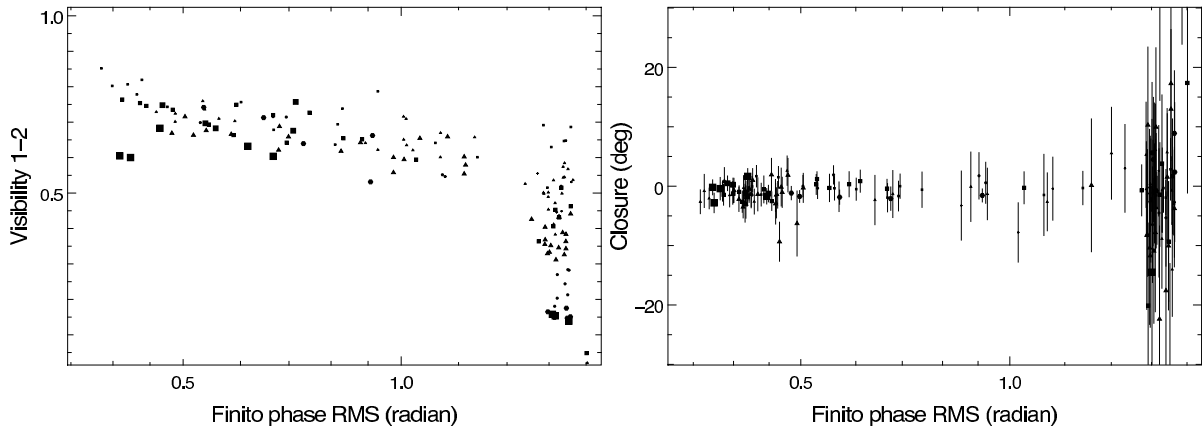

Figure 6. Observed visibilities (left) and closure-phases (right) in AMBER versus the residual of the fringe-tracking loop (RMS of the FINITO phase). RMS larger than 1.3 radian denote observations made in open loop. Symbol sizes are for the AMBER detector integration time: 0.1, 0.5, 1.0 and 5.0s (sorted by increasing symbol size). Results have been computed with the standard AMBER pipeline `amdlib`, by keeping 30% of the best frames sorted by SNR.

authors considered extremely stable atmospheric conditions allowing FINITO integration time as long as 10ms. From our knowledge, the fringe-tracking loop has never been closed in Paranal with integration times larger than 2ms, and only with atmospheric conditions considered as very good for the site (seeing smaller than 0.6as and coherence time larger than 6ms). We also think that the computation of Gai et al. assumed stable and well injected beams while it is probably not the case (focus problem on the ATs and tip-tilt residuals larger the specifications).

4.2 AMBER data quality when using FINITO

AMBER is the near-IR, 3 telescopes, spectrally dispersed beam combiner of the VLTI. The low resolution mode (R = 45) covers simultaneously the J,H and K bands ; while the medium and high resolution modes (R = 1100 and R = 10 000) possibly cover spectral ranges of 350nm and 45nm respectively. Without fringe-tracking,

the integration time should be kept smaller than the atmospheric coherence time, leading to a maximum DIT of about 100ms (DIT: Detector Integration Time, that is integration time of individual frames). In medium and high resolution mode, this strongly restricts the limiting magnitude and the spectral window size. With fringe-tracking, the full spectral window can be read and the limiting magnitude is limited by the fringe-tracker sensibility.

Figure 6 shows the AMBER visibilities and closure phase versus the fringe-tracking performance of FINITO expressed as RMS of the residual phase. AMBER data have been reduced with the standard `amdlib` pipeline, by keeping 30% best frames sorted by SNR. FINITO was running at 1kHz. Observations have been carried out in relatively good conditions: seeing~0.9as, τ_0 of 3~5ms. Looking at this plot, AMBER visibility shows a clear trend versus the FINITO performance and the gain of fringe-tracking is much more significant when using long DIT on AMBER. Yet, even when fringe-tracking is working perfectly the AMBER visibility is significantly increased by using shorter DITs. Concerning the closure phase, no bias is noticeable versus the FINITO performance. Interestingly, the closure-phase precision is highly enhanced as soon as the fringe-tracking loop is closed, even if it provides only bad performance.

From an operational point of view, the conclusions are the following: (i) If user is interested in differential visibility, phase or closure-phase, FINITO should always be used even if providing bad performance. (ii) Absolute closure-phase value is not biased by the use of FINITO or not, at least at the level we were able to check it (1deg). (iii) The absolute visibility obviously depends on the FINITO performance. Yet, it is still not clear if the transfer function stability is better or worst when using FINITO. One may consider dedicated studies based on data currently available in the ESO archive.

4.3 MIDI and FINITO operations

MIDI is the mid-infrared instrument of the VLT interferometer. It combines two beams and provides visibility measurments at different wavelengths within the N-band (8 to 13μm). MIDI was of the first instrument interfaced with FINITO, but since then it has rarely been used for scientific observations. First, most of the MIDI targets have very low fringe contrast at FINITO wavelength, often below its capability, because of the increased spatial resolution obtained at H-band compared to N-band. This is especially true for the calibration stars (on most of the scientific targets the H- and N-band fluxes originate from different components of the source, H-band being usually more compact). Secondly, with typical τ_0, the turbulence strength does not affect significantly the measure during a MIDI OPD-scan (i.e., the record of an interferogram). Anyway, and unlike AMBER, the integration time per MIDI frame (18 ms by default) is limited by the thermal background from the sky and the VLTI optics. All together, this makes the gain of fringe-tracking much less impressive on MIDI than on AMBER. Finally, MIDI is mostly limited by the quality of the measurement of the non-correlated photometric flux measured by telescope chopping, that is used to derivate the fringe visibility from the raw fringe amplitude.

5. PERSPECTIVES

5.1 Post processing the fringe-tracking data into astrophysical visibility points

The commissioning of the VLTI *Reflective Memory Network Recorder* (RMNrec) in February 2008 made possible to store the real-time FINITO, OPDC and Delay Lines data into proper FITS files. Since then, we have demonstrated the capability of post-processing the FINITO signals $C_{10}(t)$ and $C_{20}(t)$ for astronomical purpose. A simple data reduction algorithm is sufficient to recover the fringe visibility with a precision of $\pm 2.5\%$. Interestingly, the transfer-function is independent from seeing, and repeatable from one night to the other. Therefore post-processing the FINITO data provides a rough, but robust, estimation of the H-band visibility even without the observation of a calibration star close in time. As an on-sky demonstration, we were able to recover the diameters of four well-known giant stars (work being published). Moreover, formal statistical errors were of the order of 0.1% for 30s integration in a H = 2^m star with the ATs, pointing on the potential precision if all systematics bias are removed. Based on the success of this demonstration, we are now working on solution to log these data on a systematic manner and possibly deliver them to the VLTI users.
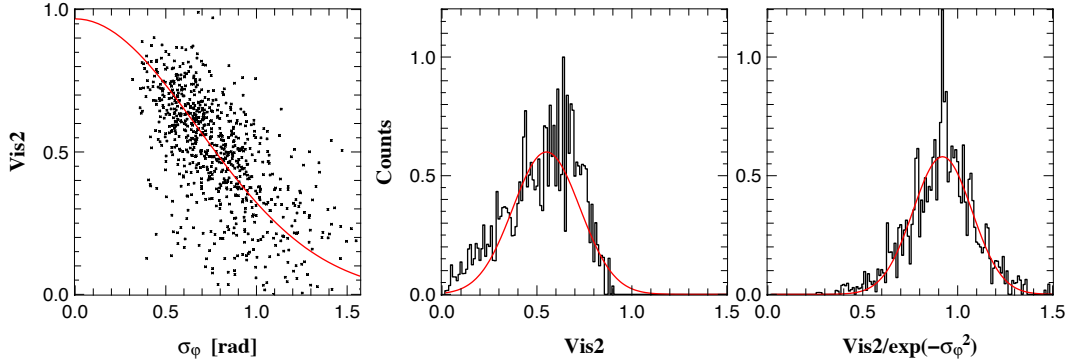
Figure 7. Left: AMBER square visibilities (vis2) versus the FINITO phase RMS (σ_ϕ) computed for each of 1000 frames of the AMBER exposure. The correlation is the so-called *jitter* effect, that is the fringe blurring due to residual fringe motion during the integration time. Red curve is a fit with the theoretical expression for the jitter attenuation factor vis2 $\propto \exp(-\sigma_\phi^2)$. Middle and Right: histogram of vis2 before and after calibration of the jitter attenuation factor (frames have been weighted by their respective SNR). Red curves are Gaussian fits to emphasize the largest skewness on the uncorrected vis2. AMBER and FINITO DITs were respectively 50ms and 1ms, and the target was a bright unresolved single star.

5.2 Using residual phase to improve AMBER data reduction

FINITO/OPDC real-time signals help the data reduction of the AMBER instrument. The AMBER integration time ranges between 25ms to 5s, values larger than 100ms being only accessible with fringe-tracking. Inside each frame, residual fringe motion reduces the observed fringe visibility by a multiplicative factor $\exp(-\sigma_\phi^2)$, where σ_ϕ is the fringe phase RMS over the integration time. This attenuation factor, sometimes called *jitter*, disturbs the observed visibility distribution and bias the final average. Practically, the use of a calibration star is supposed to remove this bias, with the strong assumption that the bias amplitude is equal for both targets. Because it uses smaller integration time (typically 0.5, 1 or 2ms), FINITO provides several phase estimation inside each AMBER frame, from which one can compute the theoretical attenuation factor and correct from it frame-to-frame. To test this idea, we recorded recently simultaneous AMBER and FINITO data on an unresolved bright target. Fig. 7 shows the obtained correlation between the computed phase RMS and the observed AMBER visibility, where the blurring effect is clearly visible and well reproduced by the theoretical form. We computed the visibility histograms before and after correcting for the jitter effect. The average visibility is enhanced toward a more realistic level (the target is unresolved, data points are already calibrated from the internal AMBER transfer function, and the VLTI transfer function alone is known to be larger than 85%), and the skewness is clearly reduced. All together, this proves the potential of the proposed technique, at least on bright and slightly resolved targets. More studies are mandatory to understand the effect on the transfer function stability and to explore how behave the jitter calibration in the low SNR regime (faintest or resolved targets).

5.3 Possible hardware improvements

Photometric residuals and fast photometric fluctuations are killers for the phase reconstruction algorithm. As first mentioned by Gai et al.,[2] FINITO would strongly benefit of replacing temporal modulation by spatial modulation. More specifically, we think best performance would be achieved with integrated-optics ABCD combiners. With such device, group-delay can possibly be estimated by slightly dispersing the H-band over few channels (as in PRIMA FSU), or by measuring alternatively the fringe contrast before and after the packet center (sometime called split-scan strategy).

Additionally, It has been proved that an instrument combining all 3 baselines pairwise can recover the input photometries without dedicated photometric extraction. Such property has been used successfully on sky during several years in the IONIC/IOTA experiment.[4] Therefore the FINITO photometric outputs can advantageously be replaced by an interferometric combination of the third pair of telescopes. Advantages are: (i) The same quantity of flux is used for each telescope pair compared to the current scheme, so no loss of performance on the already tracked baselines. (ii) The additional third baseline provides an additional, independent phase

information to keep the array co-phased, which would automatically improves the global performance. This may also reduce the number of fringe loss events. (iii) For imaging programs, fringe visibilities are hardly predictable and quickly change with time because of the super-synthesis effect. They sometimes become very small when falling exactly between the so-called visibility lobes. Being able to track on whatever pair of baselines of the telescope triangle (short-medium, short-long, medium-long), without having to reconfigure the VLTI, brings a decisive versatility for the success of these programs. (iv) Finally FINITO would be able to provides an accurate estimation of the target closure-phase in the H-band, with evident scientific complementarity with the observations made simultaneously in another band by the scientific instrument. Given the precision obtained on other interferometers using a similar concept, an accuracy better than 0.1 deg is most probably achievable.

We conclude that FINITO beam-combiner may be advantageously replaced by a 3-beam, pairwise, ABCD, integrated-optics chip. Such devices are currently being tested in laboratory, and may become available soon.

ACKNOWLEDGMENTS

REFERENCES

[1] Bonnet, H., Bauvir, B., Wallander, A., Cantzler, M., Carstens, J., Caruso, F., di Lieto, N., Guisard, S., Haguenauer, P., Housen, N., Mornhinweg, M., Nicoud, J.-L., Ramirez, A., Sahlmann, J., Vasisht, G., Wehner, S., and Zagal, J., "Enabling Fringe Tracking at the VLTI," *The Messenger* **126**, 37–+ (Dec. 2006).

[2] Gai, M., Menardi, S., Cesare, S., Bauvir, B., Bonino, D., Corcione, L., Dimmler, M., Massone, G., Reynaud, F., and Wallander, A., "The VLTI fringe sensors: FINITO and PRIMA FSU," in [*New Frontiers in Stellar Interferometry, Proc. of SPIE, Vol.me 5491. Edited by Wesley A. Traub. Bellingham, WA: The International Society for Optical Engineering, 2004., p.528*], Traub, W. A., ed., *Presented at the Society of Photo-Optical Instrumentation Engineers (SPIE) Conference* **5491**, 528–+ (Oct. 2004).

[3] Bonino, D., Gai, M., Corcione, L., and Massone, G., "Models for VLTI fringe sensor units: FINITO and PRIMA FSUs," in [*New Frontiers in Stellar Interferometry, Proceedings of SPIE Volume 5491. Edited by Wesley A. Traub. Bellingham, WA: The International Society for Optical Engineering, 2004., p.1463*], Traub, W. A., ed., *Presented at the Society of Photo-Optical Instrumentation Engineers (SPIE) Conference* **5491**, 1463–+ (Oct. 2004).

[4] Berger, J., Haguenauer, P., Kern, P. Y., Rousselet-Perraut, K., Malbet, F., Gluck, S., Lagny, L., Schanen-Duport, I., Laurent, E., Delboulbe, A., Tatulli, E., Traub, W. A., Carleton, N., Millan-Gabet, R., Monnier, J. D., and Pedretti, E., "An integrated-optics 3-way beam combiner for IOTA," in [*Interferometry for Optical Astronomy II. Edited by Wesley A. Traub. Proc. of SPIE, Vol. 4838, pp. 1099-1106.*], 1099–1106 (Feb. 2003).

---

*`http://yorick.sourceforge.net`